Commensal bacteria inhibit viral infections via a tryptophan metabolite.

Danting Jiang[1,2], Nicole Soo[3,12], Chin Yee Tan[1,4,12], Sedem Dankwa[3], Hsuan-Yuan Wang[3,5], Barbara S. Theriot[1], Amir Ardeshir[6], Nazema Y. Siddiqui[7], Koen K. A. Van Rompay[8], Kristina De Paris[9], Sallie R. Permar[3,10], Ria Goswami[3,10]* and Neeraj K. Surana[1, 4,5,11,13]*

[1]Department of Pediatrics, Duke University School of Medicine, Durham, NC, USA.

[2]Program in Computational Biology and Bioinformatics, Duke University School of Medicine, Durham, NC, USA.

[3]Department of Pediatrics, Weill Cornell Medicine, New York, NY, USA.

[4]Department of Molecular Genetics and Microbiology, Duke University School of Medicine, Durham, NC, USA.

[5]Department of Integrative Immunobiology, Duke University School of Medicine, Durham, NC, USA.

[6]Tulane National Primate Research Center, Tulane University, Covington, LA, USA.

[7]Division of Urogynecology and Reconstructive Pelvic Surgery, Department of Obstetrics and Gynecology, Duke University School of Medicine, Durham, NC, USA.

[8]California National Primate Research Center, University of California, Davis, CA, USA

[9]Department of Microbiology and Immunology, University of North Carolina, Chapel Hill, NC, USA.

[10]Drukier Institute for Children's Health, Weill Cornell Medicine, New York, NY USA.

[11]Department of Cell Biology, Duke University School of Medicine, Durham, NC, USA.

[12]These authors contributed equally

[13]Lead contact

*Correspondence: rig4007@med.cornell.edu (R.G); neil.surana@duke.edu (N.K.S)

SHORT TITLE: The gut microbiota inhibits viral infections

ABSTRACT

There is growing appreciation that commensal bacteria impact the outcome of viral infections, though the specific bacteria and their underlying mechanisms remain poorly understood. Studying a simian–human immunodeficiency virus (SHIV)-challenged cohort of pediatric nonhuman primates, we bioinformatically associated *Lactobacillus gasseri* and the bacterial family Lachnospiraceae with enhanced resistance to infection. We experimentally validated these findings by demonstrating two different Lachnospiraceae isolates, *Clostridium immunis* and *Ruminococcus gnavus*, inhibited HIV replication in vitro and ex vivo. Given the link between tryptophan catabolism and HIV disease severity, we found that an isogenic mutant of *C. immunis* that lacks the aromatic amino acid aminotransferase (ArAT) gene, which is key to metabolizing tryptophan into 3-indolelactic acid (ILA), no longer inhibits HIV infection. Intriguingly, we confirmed that a second commensal bacterium also inhibited HIV in an ArAT-dependent manner, thus establishing the generalizability of this finding. In addition, we found that purified ILA inhibited HIV infection by agonizing the aryl hydrocarbon receptor (AhR). Given that the AhR has been implicated in the control of multiple viral infections, we demonstrated that *C. immunis* also inhibited human cytomegalovirus (HCMV) infection in an ArAT-dependent manner. Importantly, metagenomic analysis of individuals at-risk for HIV revealed that those who ultimately acquired HIV had a lower fecal abundance of the bacterial ArAT gene compared to individuals who did not, which indicates our findings translate to humans. Taken together, our results provide mechanistic insights into how commensal bacteria decrease susceptibility to viral infections. Moreover, we have defined a microbiota-driven antiviral pathway that offers the potential for novel therapeutic strategies targeting a broad spectrum of viral pathogens.

INTRODUCTION

Despite recent advances in vaccines and antiviral therapeutics, viral infections pose a continued threat to humanity[1-3]. For all viruses, there exists significant heterogeneity in infection or disease outcome of exposed individuals. While some people remain uninfected, others have disease severities that span the entire spectrum from asymptomatic to fatal[4,5]. Although numerous host characteristics (e.g., age, genetics, immune status) and viral features (e.g., virulence factors, route and dose of infection) contribute to this vast interindividual variability in clinical outcomes[4,6], most of these aspects are difficult to meaningfully alter. Identifying modifiable factors that skew the response towards increased resistance to viral infections and/or their severity, particularly if effective against multiple classes of viruses, may yield novel broadly-acting antiviral therapeutics[7].

It is now clear that environmental factors, including the microbiota, also modulate susceptibility to viral infections[8-10]. Commensal bacteria can potentiate viral infectivity by the virus binding to bacterial surface polysaccharides, which help stabilize the virion[11-13]. Moreover, commensal bacteria play a fundamental role in setting the immunological tone and regulating immune responses[14,15], which provides another mechanism for influencing the severity of viral disease, especially through modulation of the interferon pathway[13,16-20]. However, the bacterial mechanisms underlying these intricate microbiota–host–virus interactions remain poorly defined[8,9]. Identification of specific commensal bacteria-derived products that decrease cellular susceptibility to viral infection will help explain the disparity in clinical outcomes of individuals with similar risk factors and exposures.

In earlier work, we noted that infant rhesus macaques varied greatly in their susceptibility to oral infection with simian-human immunodeficiency virus (SHIV)[21], a model of breast milk transmission of HIV. By correlating their susceptibility to SHIV acquisition with their fecal microbiota, we found that increased resistance was bioinformatically associated with two bacterial taxa, *Lactobacillus*

77 *gasseri* and the family Lachnospiraceae, which we then experimentally validated as inhibiting HIV
78 infection in vitro and ex vivo. Ultimately, we delineated a pathway, including the bacteria, bacterial
79 gene, bacterial metabolite, and host receptor, by which specific commensal bacteria inhibit both
80 HIV and cytomegalovirus (CMV) infections. Importantly, we used metagenomic data to confirm
81 the key aspect of our findings in individuals at-risk for HIV, thus generalizing our results to humans.
82 Taken together, our study provides mechanistic insights into how the microbiome drives
83 heterogeneous clinical outcomes resulting from viral exposures.
84
85 **RESULTS**
86 **Microbe–phenotype triangulation associated two bacterial taxa with protection against**
87 **SHIV infection**
88 To identify commensal bacteria that protect against viral infections, we leveraged samples from a
89 previously conducted study where infant rhesus macaques were orally challenged with SHIV to
90 mimic breast milk transmission of HIV[21]. In brief, newborn animals were immunized with 3 doses
91 of either a placebo or HIV gp120-based vaccine (n=12 animals/group) and, beginning at 15 weeks
92 of age (3 weeks after the final immunization), received weekly oral challenges with SHIV until they
93 became infected **(Figure 1A)**. Although the HIV vaccine did not confer protection against infection,
94 the animals exhibited drastic variability in the time to acquisition of SHIV **(Figure 1B)**[21]. Since
95 gastrointestinal tissues are one of the first sites that get infected upon oral viral transmission[22],
96 we reasoned that differences in the intestinal microbiome may contribute to the variability in time
97 to acquisition of SHIV.
98
99 Accordingly, we analyzed the fecal microbiome of these rhesus macaques at 15 weeks of age—
100 just before they began the oral SHIV challenge—to identify bacterial taxa that are associated with
101 delayed acquisition of SHIV. Inspection of the data distribution for the time to SHIV acquisition
102 revealed 3 separate clusters: animals that were infected early (≤8 challenges), late (≥20

103 challenges), or in between these time points (8–20 challenges) **(Figure 1B)**. We hypothesized
104 that taxa more abundant in the late-infected group as compared to the early-infected group may
105 be causally related to delayed infection. Given that vaccination altered the microbiota in these
106 animals[23], we initially assessed the vaccination and control groups separately. For the control
107 group of animals, there was only 1 animal in the late-infected group, which precluded our ability
108 to identify differentially abundant taxa. By comparing the microbiota in the HIV-vaccinated animals
109 that got infected early with the HIV-vaccinated animals that got infected late, we identified 4 taxa
110 that were more abundant in the late-infected animals **(Supplementary Table 1).** Applying
111 concepts of microbe–phenotype triangulation[24], we eliminated 2 of these taxa that were
112 differentially abundant in the microbiomes of early-infected animals in the HIV vaccine and control
113 groups as the abundance of these taxa are driven by the effect of vaccination without impacting
114 susceptibility to infection (**Figure 1C; Supplementary Table 1**). Ultimately, we identified two
115 taxa—*Lactobacillus gasseri* and the family Lachnospiraceae—that were bioinformatically
116 associated with delayed acquisition of SHIV **(Figure 1C–E).** Notably, *L. gasseri* has previously
117 been identified as inhibiting HIV infection in vitro[25,26], which supports the idea that our bioinformatic
118 analyses identified relevant taxa.
119

120 **Human-derived *L. gasseri* and Lachnospiraceae isolates robustly inhibit HIV infection in**
121 **vitro and ex vivo**

122 We obtained human-derived isolates of the identified bacterial taxa to experimentally validate
123 whether these bioinformatic associations also represent causal relationships. We pre-treated
124 TZM-bl luciferase reporter cells with heat-killed cultures of these bacteria for 48 hours before
125 infecting with HIV to assess their impact on HIV viral replication. To control for the potential of
126 non-specific effects due to the addition of bacteria, we compared the effects of our bacteria of
127 interest to TZM-bl cells treated with *Bacteroides fragilis*, a bacterium used as a negative control.
128 As expected, cells treated with a combination of antiretroviral drugs (ARVs) had nearly complete

129 inhibition of HIV infection, regardless of whether a CCR5- or CXCR4-tropic virus was used **(Figure**
130 **2A–B)**. While *L. gasseri* exhibited strain-dependent inhibition against HIV infection, two
131 Lachnospiraceae isolates, *Clostridium immunis* and *Ruminococcus gnavus*, robustly inhibited HIV
132 replication irrespective of virus tropism or viral clade **(Figure 2A–B** and **Supplementary Figure**
133 **1A–C)**. Importantly, both *C. immunis* and *R. gnavus* significantly inhibited HIV infection of T cells
134 present in tonsillar mononuclear cells (TMCs) isolated from HIV-naïve children (**Figure 2C**). This
135 ex vivo inhibitory activity confirms that these Lachnospiraceae isolates—but not *L. gasseri*—are
136 effective in protecting primary human immune cells from HIV infection, a finding that prompted us
137 to focus on *C. immunis* and *R. gnavus* in subsequent experiments.

138 To gain insight into the mode of action of these commensal bacteria, we performed time-
139 of-addition (TOA) assays to define which step(s) of HIV pathogenesis is impacted[27]. This TOA
140 approach assesses how long the addition of an antiviral agent can be delayed without losing its
141 efficacy. We used several reference anti-HIV drugs with known mechanisms of action to define
142 time points that reflect viral entry/fusion with the host cell, reverse transcription, and integration
143 **(Supplementary Figure 2)**. Comparing the TOA results for *R. gnavus* and *C. immunis* with that
144 of the controls, we found that *R. gnavus* inhibits the viral entry/fusion step while *C. immunis* inhibits
145 integration **(Figure 2D)**. Of note, *C. immunis* exhibited a considerable loss of inhibitory activity
146 between 0- and 8-hours post-infection. While this did not reach the threshold for statistical
147 significance, it is possible that *C. immunis* also impacts one of these earlier steps of HIV given
148 how these assays work[27,28].

149

150 **Commensal bacteria inhibit HIV infection via the ArAT gene**

151 In earlier experiments, we allowed heat-killed bacterial cells to persist with the TZM-bl cells during
152 viral infection, which makes it less clear whether the bacteria were impacting the host cells or the
153 virus. To discriminate between these possibilities, we now washed away the bacteria before
154 infecting the cells with HIV. We found that HIV infection was still inhibited in these bacteria pre-

155 treated cells **(Supplementary Figure 3)**, a finding that suggests these commensal bacteria were
156 directly affecting the host cells. We then separated the *C. immunis* culture into supernatant and
157 cell pellet fractions. While the bacterial supernatant was able to inhibit HIV infection of TZM-bl
158 cells to the same extent as the unfractionated culture, the *C. immunis* cell pellet had no activity
159 **(Figure 3A)**. Taken together, these data indicate that *C. immunis* secretes some factor(s) into the
160 supernatant which can alter cellular physiology in a way that prevents HIV infection.
161
162 It has long been appreciated that the degree of tryptophan metabolism is linked to HIV
163 pathogenesis and disease severity, with increases in the serum kynurenine:tryptophan (K/T) ratio
164 linked to progressive disease[29,30]. These studies have largely focused on host-mediated
165 catabolism of tryptophan to kynurenine by indoleamine-2,3-dioxygenase (IDO1); however, the gut
166 microbiota can also breakdown tryptophan into different metabolites through the bacterial
167 aromatic amino acid aminotransferase (ArAT)[31]. Along these lines, *C. immunis* has an ArAT gene,
168 which we hypothesized is critical for its ability to inhibit HIV infection by regulating tryptophan
169 levels. Although genetic manipulation of most commensal bacteria remains challenging[32,33], we
170 developed new genetic tools for *C. immunis* and generated an isogenic mutant (*C. immunis*ΔArAT)
171 that lacks a functional ArAT gene. Remarkably, the *C. immunis*ΔArAT mutant had greatly reduced
172 ability to inhibit HIV infection in TZM-bl cells or in primary T cells present in human TMCs
173 compared to the parental strain **(Figure 3B–C)**. TOA studies performed with the *C. immunis*ΔArAT
174 mutant demonstrated that it is able to inhibit viral entry/fusion but not any post-fusion steps
175 **(Figure 3D** and **Supplementary Figure 2)**. Given that the ArAT gene is present in diverse
176 bacteria, we reasoned that other commensal bacteria may also inhibit HIV infection in an ArAT-
177 dependent manner. Accordingly, we tested whether *Lactobacillus reuteri* and an isogenic mutant
178 deficient in ArAT were able to inhibit HIV infection. Intriguingly, while *L. reuteri* possessed inhibitory

179 activity, *L. reuteri*ΔArAT did not **(Figure 3E)**. Taken together, our data establish that commensal
180 bacteria can inhibit HIV integration via ArAT.
181
182 **Bacterial production of ILA inhibits HIV infection by activating the aryl hydrocarbon**
183 **receptor**
184 We performed untargeted metabolomics on the culture supernatant from *C. immunis* and *C.*
185 *immunis*ΔArAT to identify compounds that might explain the difference in activity. Of the 214
186 annotated metabolites, only 1—indole-3-lactic acid (ILA)—was differentially abundant between
187 the two strains, with the mutant unable to produce any ILA (**Figure 4A**). Of note, *L. reuteri* has
188 also been shown to produce ILA, in addition to indole-3-aldehyde (I3A), in an ArAT-dependent
189 manner[34,35]. We treated cells with each of these compounds to determine whether either is
190 sufficient for inhibiting HIV infection. Interestingly, we found that ILA—but not I3A—was sufficient
191 to inhibit HIV infection **(Figure 4B)**, a finding that suggests there is some specificity in terms of
192 which tryptophan catabolites have antiviral activity. Given that ILA is a known agonist of the aryl
193 hydrocarbon receptor (AhR)[31], a transcription factor that regulates expression of a broad array of
194 genes, we hypothesized that bacterial ArAT-derived ILA inhibits HIV infection by activating this
195 pathway. Indeed, the canonical AhR agonist 6-formylindolo(3,2-b)carbazole (FICZ) also inhibited
196 HIV infection **(Figure 4B)**, which demonstrates that activation of the AhR is sufficient to inhibit HIV
197 infection.
198
199 Importantly, activation of the AhR reduces viral infections by inhibiting expression of cyclin-
200 dependent kinases (Cdk) 1 and 2 along with their associated cyclins[36]. Consistent with this, we
201 found that *C. immunis* treatment of TZM-bl cells led to decreased expression of *Cdk1* with no
202 impact on *Cdk2* **(Figure 4C and 4D)**. Moreover, this effect on *Cdk1* expression was dependent
203 on the *C. immunis* ArAT being present **(Figure 4C)**. Collectively, these data strongly suggest that

204 bacterial catabolism of tryptophan into ILA inhibits HIV infection by activating the AhR and
205 decreasing *Cdk1* expression.
206
207 To determine whether these findings are relevant to human infections, we analyzed publicly
208 available fecal shotgun metagenomic data from a study that longitudinally followed an at-risk
209 population for acquisition of HIV, where only some individuals became HIV-positive[37]. Intriguingly,
210 those individuals who ultimately acquired HIV had a lower abundance of the ArAT gene before
211 becoming HIV-positive compared to those who did not acquire HIV **(Figure 4E)**. This finding
212 suggests that the bacterial ArAT gene is associated with protection against HIV in humans, which
213 strongly supports our model that bacterial ArAT-mediated metabolism of tryptophan protects
214 individuals against HIV.
215
216 **Bacterial ArAT also inhibits CMV replication**
217 We speculated this commensal bacteria–ILA–AhR pathway may be relevant in modulating the
218 susceptibility to other viruses given that activation of the AhR has been linked to the pathogenesis
219 of numerous viral infections (e.g., human cytomegalovirus [HCMV], Zika virus, influenza virus)[38,39].
220 Accordingly, we tested whether *C. immunis* can modulate HCMV infection in vitro. Remarkably,
221 *C. immunis* inhibited HCMV infection in an ArAT-dependent manner **(Figure 5A)**, which clearly
222 demonstrates that bacterial ArAT can inhibit infection from vastly divergent viruses.
223
224 **DISCUSSION**
225 Starting with infant rhesus macaques that exhibited differential susceptibility to enteral SHIV
226 infection[21], we bioinformatically identified and experimentally validated several bacterial species
227 as inhibiting HIV infection in vitro and ex vivo. Moreover, we delineated a pathway where specific
228 commensal bacteria use the ArAT to catabolize tryptophan into ILA that activates the AhR and
229 results in increased resistance against viral infections. Importantly, we leveraged metagenomic

230 data from individuals at risk for HIV infections to demonstrate our findings are generalizable to
231 humans.
232
233 Our study presents a highly effective framework to identify specific bacteria, and the underlying
234 molecular mechanisms, that are causally related to a phenotype of interest, something that
235 remains challenging to accomplish in microbiome studies[40,41]. Our successful implementation of
236 microbe-phenotype triangulation, an innovative bioinformatic discovery platform we previously
237 developed[24], to associate *L. gasseri* and the family Lachnospiraceae with increased resistance to
238 viral infection further demonstrates the utility of this approach[24,42]. Indeed, our analysis
239 independently identified *L. gasseri*, which has previously been shown to inhibit HIV infection in
240 vitro[25,26]. Moreover, our association of Lachnospiraceae with increased resistance is consistent
241 with its abundance being lower in individuals living with HIV than in healthy controls[43-47]. Similar
242 to our previous work[24], we were able to increase the specificity of our bioinformatic analyses by
243 incorporating pairwise comparisons that should not relate to the phenotype of interest. Here, we
244 were able to exclude two *Bacteroides* spp. from consideration, and we ultimately used a
245 *Bacteroides* spp. as our negative control to further demonstrate that our taxa of interest had
246 biologic effects that are not present in all bacteria.
247
248 We extended our discovery pipeline by combining it with principles of microbial pathogenesis to
249 elucidate the underlying molecular mechanism. We developed bacterial genetics for *C. immunis*,
250 a human-derived Lachnospiraceae isolate, so we could generate an isogenic mutant lacking ArAT,
251 which catalyzes the first step of tryptophan catabolism to specific indolic compounds[31].
252 Interestingly, the *C. immunis*ΔArAT mutant lacked inhibitory activity against HIV and CMV
253 infections. While this type of genetic inactivation is still infrequent in microbiome studies[40], it will
254 become more commonplace as genetic tools for manipulating commensal bacteria become more
255 advanced[48,49]. Identifying a specific gene as being critical to inhibiting viral infections enabled us

256 to investigate the abundance of the ArAT gene in shotgun metagenomic data derived from
257 relevant patient populations to quickly evaluate relevance in human disease. Taken together, we
258 have combined microbe–phenotype triangulation as a discovery platform, bacterial genetics, and
259 metagenomic analyses to elucidate the mechanism and translational relevance of microbiome-
260 mediated inhibition of viral infections.
261
262 We found that the *C. immunis* ArAT produced ILA, a microbiome-derived endogenous agonist for
263 the AhR signaling pathway that ultimately leads to protection against viral infections. The AhR is
264 strongly linked to viral pathogenesis[39], though there is ongoing controversy whether the AhR
265 pathway promotes or restrains these infections[38,39]. These discrepancies may relate to the role of
266 AhR signaling varying in a virus-[39,50-53], cell type-[50,54,55], and ligand-specific manner[54,56,57].
267 Consistent with these findings, we found that ILA—but not I3A—robustly suppresses viral
268 infection even though both are AhR agonists that are produced in an ArAT-dependent manner[31].
269 It is likely that other microbiome-derived AhR agonists may similarly inhibit viral infections.
270
271 In addition to microbiome-mediated tryptophan catabolism, the host can also metabolize
272 tryptophan directly, with generation of kynurenine by IDO1 being a common pathway. The level
273 of kynurenine, often reported as the ratio of kynurenine to tryptophan (K/T ratio), is linked to more
274 severe viral infections[29,30,58,59]. Although kynurenine does not have direct AhR binding activity, it is
275 an AhR pro-ligand that requires chemical conversions to act as an AhR agonist[60]. While
276 kynurenine can modulate the immune system in an AhR-dependent manner[61-63], it is less clear
277 whether it directly impacts the severity of viral infections in vivo[64]. We speculate that the clinical
278 observations linking kynurenine to more severe viral disease may be driven by differences in
279 microbiome-mediated tryptophan catabolism, with increased kynurenine levels serving as a proxy
280 for lower levels of tryptophan-catabolizing bacteria. Metabolism of tryptophan by commensal

281 bacteria, which occurs in the intestinal lumen prior to absorption of tryptophan, reduces the
282 amount of tryptophan available to the host for conversion into kynurenine.
283
284 It is notable that commensal bacteria-derived ILA can inhibit both HIV, a retrovirus, and CMV, a
285 DNA virus, given the vast differences in their underlying biology. These effects do not require
286 modulation of the immune system as the effects are also present in epithelial cell line-based
287 experiments, a finding that suggests the bacteria are altering cellular physiology in a way that
288 affects viral pathogenesis. AhR activation is known to modulate expression of numerous genes,
289 including repressing expression of *Cdk1* and *Cdk2*[36]. Along these lines, we found that cells treated
290 with *C. immunis* have reduced expression of *Cdk1* in an ArAT-dependent manner, a finding that
291 helps mechanistically explain how commensal bacteria-generated ILA leads to protection against
292 viral infection. Given that CDK1 normally phosphorylates SAMHD1[65], thereby inhibiting its
293 dNTPase activity[65,66], treatment with *C. immunis* likely leads to an increase in active, non-
294 phosphorylated SAMHD1 and a concomitant reduction in the dNTP pool available for viral DNA
295 synthesis, similar to what has been previously demonstrated for FICZ[36]. We speculate that *C.*
296 *immunis* and other ArAT-expressing commensal bacteria inhibit viral infection for a broad array of
297 viruses—beyond just HIV and CMV—since the underlying mechanism revolves around the
298 availability of dNTPs necessary for viral replication.
299
300 Overall, by starting with the observation that infant rhesus macaques had variable susceptibility
301 to SHIV challenges, we defined a mechanistic pathway for how the microbiota influences
302 susceptibility to viral infections. We used microbe–phenotype triangulation to associate bacterial
303 taxa with delayed acquisition, in vitro and ex vivo experiments to validate our bioinformatic
304 findings, bacterial genetics to clarify the critical role of the ArAT gene in multiple bacteria, and
305 metagenomic analyses of an at-risk patient population to demonstrate the translational relevance
306 of our findings. Taken together, our results provide a mechanistic basis for the significant

307 heterogeneity in clinical outcomes of virus-exposed individuals. More broadly, our findings offer
308 the potential for a microbiome-based therapeutic to treat and/or prevent viral infections.
309
310 **METHODS.**
311 **Microbe–phenotype triangulation to identify protective taxa in SHIV-challenged monkeys.**
312 We obtained data from a previous study involving a cohort of infant rhesus macaques that were
313 challenged with simian–human immunodeficiency virus (SHIV) and exhibited variable levels of
314 susceptibility to infection[21]. As previously described, animals were immunized with either a HIV
315 gp120-based vaccine or control vaccine at 0, 6, and 12 weeks of age (*n* = 12/group) before they
316 were orally challenged with SHIV weekly beginning at 15 weeks of age[21]. The fecal microbiome
317 of these animals at 15 weeks of age has been previously described[23]. Briefly, they were generated
318 by 16S rRNA gene sequencing, with data processed by the standard DADA2-based pipeline.
319 Identification of differentially abundant taxa for the pairwise comparisons used in the microbe–
320 phenotype triangulation approach was accomplished in R using DESEq2[67], with default
321 thresholds. Taxa present in <50% of animals in both groups of the comparison were not included
322 in the analysis.
323
324 **Bacterial strains.** *C. immunis*, *R. gnavus* (ATCC 29149), and *B. fragilis* (NCTC 9343) were
325 obtained from Dennis Kasper (Harvard University)[24]. All *L. gasseri* strains were isolated from
326 catheterized urine samples of healthy women. *L. reuteri* 100-23 (wild-type and ΔArAT mutant)
327 were obtained from Luisa Cervantes-Barragan (Emory University)[68]. *C. immunis*, *R. gnavus*, and
328 *B. fragilis* were grown in peptone–yeast–glucose (PYG) broth (Anaerobe Systems) or brain heart
329 infusion-supplemented (BHI-S) broth (ATCC medium 1293). *Lactobacillus* strains were grown in
330 De Man, Rogosa and Sharpe (MRS) broth (Sigma). All bacterial strains were grown in an
331 anaerobic chamber (Coy laboratories) with 2.5% H_2 and 0 ppm O_2 at 37 °C. Serial dilutions of
332 overnight cultures of the bacterial isolates were plated to enumerate the colony-forming units

333 (CFU). Cultures were heat-killed at 65 °C for 20 mins, aliquoted, and frozen at -80 °C until further
334 use. To separate the bacterial supernatant from the bacterial cells, the heat-killed cultures were
335 centrifuged at 10,000 rpm for 5 min. The culture supernatant was collected, and the bacterial
336 pellet was washed twice with 1X PBS and resuspended in an equivalent volume of TZM-bl
337 maintenance media.
338
339 **Cell lines and primary cells.** TZM-bl luciferase reporter cells (BEI Resources, ARP-8129) and
340 human embryonic kidney-293T (HEK-293T) cells (ATCC CRL-3216) were cultured in Dulbecco's
341 Modified Eagle Medium (DMEM) (Gibco), with 10% heat-inactivated FBS (Millipore Sigma), 1%
342 penicillin-streptomycin (Gibco), and 25 mM of HEPES (Gibco). Human retinal pigment epithelial
343 (ARPE) cells (ATCC CRL-2302) were cultured in DMEM-F12 (Gibco), with 10% FBS, and 1%
344 penicillin-streptomycin (Gibco). Human foreskin fibroblast (HFF-1) cells (ATCC SCRC-1041) were
345 maintained in DMEM (Gibco) with 20% FBS, 2mM L-glutamine, 25mM HEPES, 1% Pen-Strep,
346 and 50 µg/ml Gentamicin. All cell lines and primary cells were cultured at 37ºC in a humidified
347 incubator with 5% CO_2.
348
349 Tonsil tissues removed during routine tonsillectomy from HIV naïve children (<15 years of age)
350 were obtained through Weill Cornell Medicine Department of Pathology and Laboratory Medicine.
351 The use of tonsil specimens for this study was reviewed and determined to be exempt from human
352 subject research by the Weill Cornell Medicine Institutional Review Board (IRB); informed consent
353 was therefore not required (Protocol # 21-08023851). Tonsil tissues were received within 1-3
354 hours of surgery; washed and minced in RPMI 1640 (Gibco) containing 1% antibiotic/antimycotic
355 (Gibco), 50µg/ml Gentamicin (Gibco), 10 µg/ml of cephalothin (Sigma-Aldrich), and 5 µg/ml of
356 fluconazole (Sigma-Aldrich); and tonsillar mononuclear cells (TMCs) were isolated by filtering
357 tonsillar tissue pieces through a 70-µm mesh filter, followed by density gradient centrifugation
358 using Ficoll-Paque PLUS (GE Healthcare), as previously described[69].

359

360 **Small molecular compounds and antibodies.** Antiretroviral (ARV) drugs zidovudine (Catalog #
361 PHR1292), lamivudine (Catalog # L1295), and nevirapine (Catalog # PHR1757) were purchased
362 from Millipore Sigma and reconstituted in DMSO. A triple-drug ARV cocktail consisting of 10μg/μL
363 zidovudine, 10μg/μL lamivudine, and 1μg/μL nevirapine was used. CH-223191 (Catalog # C8124),
364 DL-Indole-3-lactic acid (ILA, Catalog # I5508), Indole-3-carboxaldehyde (I3A, catalog # 129445)
365 and 6-Formylindolo[3,2-b]carbazole (FICZ, catalog # SML1489) were purchased from Millipore
366 Sigma and reconstituted in DMSO, according to the manufacturer's instructions. HIV replication
367 inhibitors (enfuvirtide, zidovudine, and raltegravir) used for the TOA assays were purchased from
368 MedChemExpress and reconstituted in DMSO according to the manufacturer's instructions. HIV
369 gp120 CD4-binding site-specific monoclonal antibody VRC01 was obtained from BEI Resources
370 (Catalog #: ARP-12033). Anti-CMV immune-globulin, Cytogam, was obtained from CSL Behring
371 Healthcare (NDC code: 49591-532-51).

372

373 **Virus propagation and titration.** The HIV-1 pNL4-3 based CXCR4-tropic GFP reporter virus
374 HIV_{NLGI} and CCR5-tropic GFP reporter virus HIV_{JRFL} have been described previously[70]. Viral
375 stocks were generated by transfecting HIV_{NLGI} and HIV_{JRFL} plasmids in HEK 293T cells using
376 JetPrime transfection reagent (Polyplus transfection, Catalog # 101000015). 48 hours after
377 transfection, the culture supernatant containing virus was harvested, filtered, and concentrated
378 using a 20% sucrose cushion and ultracentrifugation at 23,000 rpm for 2 hr. The viral stock was
379 then resuspended in 1X PBS, aliquoted, and stored at -80º C. Viral titers were determined using
380 a commercial p24 ELISA kit (PerkinElmer, Catalog # NEK050B001KT), according to the
381 manufacturer's instructions.

382

383 Subtype B (TRO.11), C (HIV_25710-2.43), and CRF07 (BJOX002000.03.2)[71] HIV-1 envelope
384 pseudoviruses were produced as previously described[72]. Briefly, 4 μg of each of the 3 HIV-

envelope expression plasmids were co-transfected with 8 µg of backbone plasmid pSG3ΔEnv in HEK 293T cells using FuGene 6 transfection reagent (Promega, catalog # E5911). Virus was harvested 48 h post-transfection, filtered, and stored at −80°C with 20% FBS in the freezing media. Pseudovirus titers were determined by infecting TZM-bl-luciferase reporter cell lines and estimating 50% tissue culture infectious dose ($TCID_{50}$) using the Bright-Glo luminescence reporter gene assay system (Promega)[73] as directed by the manufacturer.

To produce GFP-tagged HCMV-AD169r-BAC human cytomegalovirus (HCMV) strain, GFP-tagged AD169r HCMV BAC clone (AD169r-GFP BAC) and the CMV pp71 plasmids[74,75] (kind gifts from Dr. Eain Murphy, Upstate Medical University) were co-transfected in HFF-1 cells using the Lipofectamine™ 3000 Transfection Reagent (ThermoFisher Scientific, catalog # L3000001), according to manufacturer's instructions. Upon development of virus-induced cytopathic effect (CPE) and GFP expression (~7–10 days post-transfection), the virus was harvested, propagated twice in ARPE-19 cells, and concentrated using ultracentrifugation at 50,000 *g* for 90 minutes at 4 ºC. For determining HCMV stock titers, ARPE-19 cells were seeded in 96 wells plates (20,000 cells/well) and incubated with the virus for 7 days, before estimating viral titers using HCMV neutralization assay as described previously[76].

HIV infection and treatment of TZM-bl cells. 10^4 TZM-bl-luciferase reporter cells were seeded per well in a 96-well plate and incubated for 24 hrs. To evaluate the efficacy of heat-killed bacteria pre-treatment in suppressing HIV replication, TZM-bl cells were treated every 24 hours with the equivalent of ~10^6 CFU of unfractionated heat-killed bacteria, washed bacterial cells, or culture supernatant. Cells pre-treated for 48 hours were either washed twice with PBS or not washed at all before being infected with 5ng p24 equivalent HIV_{NLGI} or HIV_{JRFL}. Cells were treated with an ARV cocktail as a positive control. 48 hours post-HIV infection, viral replication was quantified using the luciferase reporter assay described above. After subtracting background luminescence,

411 HIV replication was calculated by dividing these background-corrected luminescence values by
412 that of the negative control (generally, cells treated with *B. fragilis*), with values expressed as a
413 percentage. Percent inhibition of HIV replication was calculated as 100 minus the HIV replication.
414
415 To evaluate the efficacy of treatment with heat-killed bacteria or small molecular inhibitors in
416 modulating HIV replication, TZM-bl cells were incubated with HIV_{NLGI} (5ng p24 equivalent), HIV_{JRFL}
417 (5ng p24 equivalent), TRO.11 ($TCID_{50}$: 2223.05), HIV_25710-2.43 ($TCID_{50}$: 2344.05), or
418 BJOX002000.03.2 ($TCID_{50}$: 3493.85), and 10^6 CFU equivalent of heat-killed bacteria or 1 nM of
419 small molecular inhibitors (3-ILA, I3A, or FICZ) for 26 hours. Viral infection was quantified using
420 luciferase reporter assay as described above.
421
422 **Time-of-addition assay.** 10^4 TZM-bl-luciferase reporter cells were seeded per well in a 96-well
423 plate and incubated for 24 hrs, after which they were incubated with 5 ng p24 equivalent HIV_{NLGI}.
424 After 1 hr, the virus-containing supernatant was removed, cells were washed twice with DPBS,
425 and fresh media was added. HIV-infected cells were then treated with either DMSO (as a negative
426 control), 1 μM of enfuvirtide, 1 μM of zidovudine, 1 μM of raltegravir, 2.5 μg of VRC01, or 10^5 CFU
427 of heat-killed bacteria at 0, 2, 4, 6, 8, 10, or 12 hours. The degree of viral infection was quantitated
428 at 26 hours post-HIV infection using the luciferase reporter assay described above.
429
430 **Bacterial treatment of HIV-infected TMCs.** Tonsillar mononuclear cells (TMCs) were
431 resuspended in RPMI 1640 (Gibco), supplemented with 10% FBS, 1X antibiotic/antimycotic
432 mixture (Gibco), 1 mM of sodium pyruvate (Sigma-Aldrich), and 1X non-essential amino acid
433 mixture (Gibco). Wells in a flat-bottom 96-well plate were loaded with 10^6 TMCs, infected with 250
434 ng p24-equivalent of GFP-tagged HIV_{NLGI}, and treated with either heat-killed bacteria or the same
435 ARV cocktail described above. Plates were then centrifuged at 1200*g* for 2hrs to help synchronize

436 infection. After 48 hours, TMCs were stained for flow cytometry-based detection of GFP
437 expression.
438
439 **Flow cytometric analysis of HIV-infected TMCs.** Suspensions of ~10^6 HIV-infected TMCs in
440 PBS with 1% FBS were incubated with BV711 anti-human CD3 antibody (Biolegend, catalog #
441 300464) at 4ºC for 30 min, after which cells were washed twice with PBS. The cells were then
442 incubated at 4ºC with LIVE/DEAD Fixable Aqua Dead Cell Stain Kit (Thermo Fisher Scientific,
443 catalog # L34957) for 30 minutes. Following incubation and washing with 1X PBS, the cells were
444 fixed using 10% formalin. The stained TMCs were analyzed on an LSRFortessa (BD Biosciences)
445 using BD FACS Diva software. Data were analyzed with FlowJo software version 10.8.1 (Tree
446 Star, Inc). The percentage of live $CD3^+$ T cells infected with GFP-tagged HIV was reported.
447
448 ***Cdk1* and *Cdk2* expression analysis.** 2 x 10^5 TZM-bl luciferase reporter cells were incubated
449 with ~10^6 CFU of heat-killed bacteria and infected with 5ng p24-equivalent HIV_{NLGI} virus. 24 hr
450 post-infection, cellular RNA was extracted using the RNeasy mini kit (Qiagen). cDNA was
451 synthesized using SuperScript™ III First-Strand Synthesis System (Thermo Fisher) following the
452 manufacturer's instructions. cDNA was amplified using TaqMan gene expression mastermix
453 (Thermo Fisher) and TaqMan Gene Expression Assays (Applied Biosystems) for *Gapdh*
454 (HS02786624_g1), *Cdk1* (Hs00938777_m1), and *Cdk2* (Hs1548894_m1). The thermal cycling
455 steps were 50°C for 2 min, 95°C for 10 min, and 40 cycles of 95°C for 15 s and 60°C for 1 min.
456 qPCR was performed on a QuantStudio 7 Flex real time PCR machine (ThermoFisher Scientific).
457 Each sample was run in duplicate and relative quantification was performed by normalization to
458 GAPDH.
459
460 **Generation of *C. immunis*ΔArAT.** We used homologous recombination to disrupt the ArAT gene
461 in *C. immunis*, using pMTL82151, one of the ClosTron plasmids[77], as a suicide vector. We used

462 the Q5 High-Fidelity DNA polymerase (NEB) to PCR amplify the *ermB* gene that provides
463 resistance to erythromycin (using pMTL83251 as the template) and two 800 bp regions
464 (separated by 80 bp) that flanked the *C. immunis* ArAT target site (representing left and right
465 homology arms), using genomic DNA from *C. immunis* as the template. PCR primers used are as
466 follows:
467 ArAT Left F: gctcggtacccggggatcctCTCTGACTGTATTCTATGAC;
468 ArAT Left R: cttcggccggGTCTTTCCGTTTATTTTCTC;
469 ArAT Right F: gaatgtgtttTCCTGGAAAAGAAGGAAAAAG;
470 ArAT Right R: agcttgcatgtctgcaggccCGGCATGAAAAATCCCAG;
471 ErmB F: acggaaagacCCGGCCGAAGCAAACTTAAG;
472 ErmB R: ttttccaggaAAACACATTCCCTTTAGTAACGTG
473
474 These three PCR products were digested with XbaI and XhoI and cloned into XbaI- and XhoI-
475 digested pMTL82151 plasmid using HiFi assembly (NEB). Electrocompetent *E. coli* S17λPir was
476 transformed with the ligation mixture, which generated S17λPir:pMTL82151ΔArAT. This strain
477 was used to transfer pMTL82151ΔArAT into *C. immunis* using standard conjugation methods.
478 Briefly, overnight cultures of *E. coli* donors and *C. immunis* recipients were mixed at a 10:1 donor-
479 to-recipient ratio. Multiple aliquots (30 μl) of the mixture were spotted onto a BHI-S agar plate and
480 incubated anaerobically at 37 °C. After 24–48 h, the total growth on each plate was collected,
481 resuspended in fresh media, and grown on BHI-S plates containing erythromycin (500 μg/ml) and
482 colistin (10 μg/ml). To confirm that the plasmid was not present in *C. immunis*, the culture was
483 also grown on BHI-S plates containing colistin (10 μg/ml) and chloramphenicol (12.5 μg/ml),
484 against which the plasmid backbone confers resistance. Erythromycin-resistant colonies of *C.*
485 *immunis* were confirmed to harbor the insertion of the *ermB* gene and expected 80-bp deletion in
486 ArAT by PCR and Sanger sequencing.

487

488 To validate the loss-of-function of *C. immunis*ΔArAT, overnight cultures of wildtype *C. immunis*
489 and *C. immunis*ΔArAT were grown in PYG and pelleted to obtain cell-free supernatants.
490 Untargeted metabolomics of the respective supernatants was performed via GC-MS at the Duke
491 Molecular Physiology Institute.

492

493 **Analysis of ArAT abundances in individuals at-risk for HIV.** We downloaded a publicly
494 available shotgun metagenomic dataset from the mSTUDY cohort that includes an at-risk
495 population followed longitudinally for the acquisition of HIV (*n=29*)[37]. We trimmed sequence reads
496 and removed host decontamination using KneadData. Forward and reverse reads that passed
497 quality control (paired and unpaired) were concatenated and fed into the HUMAnN 3 pipeline for
498 functional profiling as UniRef90 gene families[78]. To identify homologs of the ArAT gene, we used
499 the *C. immunis* and *L. reuteri* ArAT gene sequences to search for UniRef90 entries in the UniProt
500 Knowledgebase[79], setting a similarity threshold of ⩾30%. We used the grep UNIX command to
501 extract the abundance of these ArAT homologs from the library-depth normalized UniRef90 gene
502 family abundance table, and we summed their abundances. Any homologs identified by both the
503 *C. immunis* and *L. reuteri* ArAT gene sequence were only counted once.

504

505 **Bacterial treatment of HCMV-infected ARPE cells.** The efficacy of *C. immunis* and *C.*
506 *immunis*ΔArAT to modulate human cytomegalovirus (HCMV) replication was assessed by
507 performing the HCMV neutralization assay as previously described[76]. Briefly, ARPE cells (5000
508 cells/well) were seeded in 384-well black plates with clear bottoms (Corning) and cultured for 24
509 hours. ARPE cell monolayers were then incubated with GFP-tagged HCMV-AD169r-BAC virus
510 strain at a multiplicity of infection (MOI) of 1.5 along with either heat-killed bacteria or 0.625 mg/mL
511 of anti-CMV immune globulin. After 48 hrs, cell culture media was aspirated and cells were fixed

512 with 10% formalin at room temperature for 15 min. Fixed cells were washed twice with PBS + 0.1%
513 Tween 20 and incubated with 1:1000 mouse anti-HCMV IE-1 monoclonal antibody (Millipore,
514 Catalog No: MAB810R, clone 8B1.2) in staining buffer (Dulbecco's PBS [DPBS] containing 1%
515 FBS and 0.3% Triton X-100) for 1 hr at RT. After subsequent washing, cells were stained with
516 goat anti-mouse IgG-AF488 (Abcam; Catalog No: ab150113) at 1:1000 dilution for 1hr at RT. After
517 further washing, the cell nucleus was stained with 1:1000 DAPI (4',6'-diamidino-2-phenylindole;
518 Invitrogen; Catalog No: D1306) nuclear stain for 10 minutes at RT. DAPI-positive (indicative of
519 total cells) and AF488-positive cell counts (indicative of HCMV-infected cells) were measured
520 using ImageXpress Pico Automated Cell Imaging System (Molecular Devices), and the
521 percentage of HCMV-positive cells of total cells was computed.
522
523 **Statistical Analysis.** Prism 10 (GraphPad Software) was used for all statistical analyses, except
524 for Benjamini-Hochberg correction of one-sample t-tests, which was done in R (version 4.2.2).
525 The specific statistical tests used are detailed in each figure legend.
526
527 **ACKNOWLEDGEMENTS**. This work was supported by Gilead Sciences Research Scholar's
528 Program in HIV (RG), National Institutes of Health grants P01 AI117915 (KVR, KDP, SRP) and
529 P01 AI178377 (KVR, KDP, SRP, RG, NKS), a pilot award from the Duke Center for AIDS Research
530 (CFAR; P30 AI064518) and Duke Microbiome Center (NKS), and The Office of Research
531 Infrastructure Programs/OD grant P51OD011107 to the CNPRC. DJ received funding from the
532 Duke CFAR Summer Internship program (R25 AI140495). The funders had no role in study design,
533 data collection and interpretation, or the decision to submit the work for publication. The content
534 is solely the responsibility of the authors. We thank the Duke Microbiome Core Facility for
535 performing the DNA extractions, quality control, and preparing the 16S rRNA gene sequencing
536 library; the Duke Sequencing and Genomic Technologies Shared Resource for sequencing the
537 16S rRNA gene library; the Duke Compute Cluster for providing the high-performance parallel

computing hardware used in bioinformatic analysis of sequencing data; and the Metabolomics/Proteomics Core at the Duke Molecular Physiology Institute for conducting the metabolomics analysis.

AUTHORS CONTRIBUTIONS.

Conceptualization: D.J., R.G. and N.K.S.

Data curation: D.J.

Formal analysis: D.J.

Funding acquisition: K.K.A.V.R., K.D.P., and S.R.P., R.G., and N.K.S.

Investigation: D.J., N.S., C.Y.T., S.D., H.Y.W., B.S.T. and R.G.

Resources: N.Y.S., A.A., K.K.A.V.R., K.D.P., and S.R.P.

Supervision: R.G. and N.K.S.

Writing – original draft: D.J., N.S., C.Y.T., R.G. and N.K.S.

Writing – review & editing: all authors.

COMPETING INTERESTS. S.R.P serves as a consultant for Merck, Moderna, Pfizer, Hoopika, Dynavax, and GSK on their CMV vaccine programs, and has led sponsored research programs with Merck and Moderna on CMV vaccines. DJ, CYT, SRP, RG, and NKS are inventors on a patent application submitted by Duke University that covers the therapeutic use of ArAT-expressing bacteria and their metabolites in viral infections. Other authors have no conflict of interest to disclose.

559 **REFERENCES.**

560

561 1. Casanova, J.-L., and Abel, L. (2021). Mechanisms of viral inflammation and disease in
562 humans. Science *374*, 1080-1086. 10.1126/science.abj7965.

563 2. Baker, R.E., Mahmud, A.S., Miller, I.F., Rajeev, M., Rasambainarivo, F., Rice, B.L.,
564 Takahashi, S., Tatem, A.J., Wagner, C.E., Wang, L.-F., et al. (2022). Infectious disease in
565 an era of global change. Nature Reviews Microbiology *20*, 193-205. 10.1038/s41579-021-
566 00639-z.

567 3. Morens, D.M., and Fauci, A.S. (2020). Emerging Pandemic Diseases: How We Got to
568 COVID-19. Cell *182*, 1077-1092. 10.1016/j.cell.2020.08.021.

569 4. Casanova, J.-L. (2015). Human genetic basis of interindividual variability in the course of
570 infection. Proceedings of the National Academy of Sciences *112*, E7118-E7127.
571 10.1073/pnas.1521644112.

572 5. Arons, M.M., Hatfield, K.M., Reddy, S.C., Kimball, A., James, A., Jacobs, J.R., Taylor, J.,
573 Spicer, K., Bardossy, A.C., Oakley, L.P., et al. (2020). Presymptomatic SARS-CoV-2
574 Infections and Transmission in a Skilled Nursing Facility. N. Engl. J. Med. *382*, 2081-2090.
575 10.1056/NEJMoa2008457.

576 6. Virgin, H.W. (2007). In vivo veritas: pathogenesis of infection as it actually happens. Nat.
577 Immunol. *8*, 1143-1147. 10.1038/ni1529.

578 7. Karim, M., Lo, C.-W., and Einav, S. (2023). Preparing for the next viral threat with broad-
579 spectrum antivirals. The Journal of Clinical Investigation *133*. 10.1172/JCI170236.

580 8. Pfeiffer, J.K., and Virgin, H.W. (2016). Transkingdom control of viral infection and immunity
581 in the mammalian intestine. Science *351*, aad5872. 10.1126/science.aad5872.

582 9. Tan, C.Y., Ramirez, Z.E., and Surana, N.K. (2021). A Modern-World View of Host-
583 Microbiota-Pathogen Interactions. J. Immunol. *207*, 1710-1718.
584 10.4049/jimmunol.2100215.

585 10. Campbell, D.E., Li, Y., Ingle, H., and Baldridge, M.T. (2023). Impact of the Microbiota on
586 Viral Infections. Annu Rev Virol *10*, 371-395. 10.1146/annurev-virology-111821-115754.
587 11. Kane, M., Case, L.K., Kopaskie, K., Kozlova, A., MacDearmid, C., Chervonsky, A.V., and
588 Golovkina, T.V. (2011). Successful transmission of a retrovirus depends on the commensal
589 microbiota. Science *334*, 245-249. 10.1126/science.1210718.
590 12. Robinson, C.M., Jesudhasan, P.R., and Pfeiffer, J.K. (2014). Bacterial lipopolysaccharide
591 binding enhances virion stability and promotes environmental fitness of an enteric virus.
592 Cell Host Microbe *15*, 36-46. 10.1016/j.chom.2013.12.004.
593 13. Kuss, S.K., Best, G.T., Etheredge, C.A., Pruijssers, A.J., Frierson, J.M., Hooper, L.V.,
594 Dermody, T.S., and Pfeiffer, J.K. (2011). Intestinal microbiota promote enteric virus
595 replication and systemic pathogenesis. Science *334*, 249-252. 10.1126/science.1211057.
596 14. Backhed, F., Ley, R.E., Sonnenburg, J.L., Peterson, D.A., and Gordon, J.I. (2005). Host-
597 bacterial mutualism in the human intestine. Science *307*, 1915-1920.
598 10.1126/science.1104816.
599 15. Surana, N.K., and Kasper, D.L. (2014). Deciphering the tete-a-tete between the microbiota
600 and the immune system. J. Clin. Invest. *124*, 4197-4203. 10.1172/JCI72332.
601 16. Stefan, K.L., Kim, M.V., Iwasaki, A., and Kasper, D.L. (2020). Commensal Microbiota
602 Modulation of Natural Resistance to Virus Infection. Cell *183*, 1312-1324.e1310.
603 https://doi.org/10.1016/j.cell.2020.10.047.
604 17. Steed, A.L., Christophi, G.P., Kaiko, G.E., Sun, L., Goodwin, V.M., Jain, U., Esaulova, E.,
605 Artyomov, M.N., Morales, D.J., Holtzman, M.J., et al. (2017). The microbial metabolite
606 desaminotyrosine protects from influenza through type I interferon. Science *357*, 498-502.
607 10.1126/science.aam5336.
608 18. Baldridge, M.T., Nice, T.J., McCune, B.T., Yokoyama, C.C., Kambal, A., Wheadon, M.,
609 Diamond, M.S., Ivanova, Y., Artyomov, M., and Virgin, H.W. (2015). Commensal microbes

610 and interferon-lambda determine persistence of enteric murine norovirus infection.
611 Science *347*, 266-269. 10.1126/science.1258025.
612 19. Van Winkle, J.A., Peterson, S.T., Kennedy, E.A., Wheadon, M.J., Ingle, H., Desai, C.,
613 Rodgers, R., Constant, D.A., Wright, A.P., Li, L., et al. (2022). Homeostatic interferon-
614 lambda response to bacterial microbiota stimulates preemptive antiviral defense within
615 discrete pockets of intestinal epithelium. eLife *11*. 10.7554/eLife.74072.
616 20. Wirusanti, N.I., Baldridge, M.T., and Harris, V.C. (2022). Microbiota regulation of viral
617 infections through interferon signaling. Trends in Microbiology *30*, 778-792.
618 10.1016/j.tim.2022.01.007.
619 21. Curtis, A.D., 2nd, Saha, P.T., Dennis, M., Berendam, S.J., Ramasubramanian, P., Cross,
620 K.A., Alam, S.M., Ferrari, G., Kozlowski, P.A., Fouda, G.G., et al. (2022). Vaccine-Induced,
621 High-Magnitude HIV Env-Specific Antibodies with Fc-Mediated Effector Functions Are
622 Insufficient to Protect Infant Rhesus Macaques against Oral SHIV Infection. mSphere *7*,
623 e0083921. 10.1128/msphere.00839-21.
624 22. John-Stewart, G., Mbori-Ngacha, D., Ekpini, R., Janoff, E.N., Nkengasong, J., Read, J.S.,
625 Van de Perre, P., and Newell, M.L. (2004). Breast-feeding and Transmission of HIV-1. J
626 Acquir Immune Defic Syndr *35*, 196-202. 10.1097/00126334-200402010-00015.
627 23. Jiang, D., Goswami, R., Dennis, M., Heimsath, H., Kozlowski, P.A., Ardeshir, A., Van
628 Rompay, K.K.A., De Paris, K., Permar, S.R., and Surana, N.K. (2023). Sutterella and its
629 metabolic pathways positively correlate with vaccine-elicited antibody responses in infant
630 rhesus macaques. Front Immunol *14*, 1283343. 10.3389/fimmu.2023.1283343.
631 24. Surana, N.K., and Kasper, D.L. (2017). Moving beyond microbiome-wide associations to
632 causal microbe identification. Nature *552*, 244-247. 10.1038/nature25019.
633 25. Nahui Palomino, R.A., Zicari, S., Vanpouille, C., Vitali, B., and Margolis, L. (2017). Vaginal
634 Lactobacillus Inhibits HIV-1 Replication in Human Tissues Ex Vivo. Front Microbiol *8*, 906.
635 10.3389/fmicb.2017.00906.

636 26. Nahui Palomino, R.A., Vanpouille, C., Laghi, L., Parolin, C., Melikov, K., Backlund, P., Vitali,
637 B., and Margolis, L. (2019). Extracellular vesicles from symbiotic vaginal lactobacilli inhibit
638 HIV-1 infection of human tissues. Nat Commun *10*, 5656. 10.1038/s41467-019-13468-9.
639 27. Daelemans, D., Pauwels, R., De Clercq, E., and Pannecouque, C. (2011). A time-of-drug
640 addition approach to target identification of antiviral compounds. Nat Protoc *6*, 925-933.
641 10.1038/nprot.2011.330.
642 28. Callegaro, S., Perrone, R., Scalabrin, M., Doria, F., Palù, G., and Richter, S.N. (2017). A
643 core extended naphtalene diimide G-quadruplex ligand potently inhibits herpes simplex
644 virus 1 replication. Scientific Reports *7*, 2341. 10.1038/s41598-017-02667-3.
645 29. Huengsberg, M., Winer, J.B., Gompels, M., Round, R., Ross, J., and Shahmanesh, M.
646 (1998). Serum kynurenine-to-tryptophan ratio increases with progressive disease in HIV-
647 infected patients. Clin. Chem. *44*, 858-862.
648 30. Murray, M.F. (2003). Tryptophan depletion and HIV infection: a metabolic link to
649 pathogenesis. Lancet Infect. Dis. *3*, 644-652. 10.1016/s1473-3099(03)00773-4.
650 31. Roager, H.M., and Licht, T.R. (2018). Microbial tryptophan catabolites in health and
651 disease. Nature Communications *9*, 3294. 10.1038/s41467-018-05470-4.
652 32. Waller, M.C., Bober, J.R., Nair, N.U., and Beisel, C.L. (2017). Toward a genetic tool
653 development pipeline for host-associated bacteria. Curr. Opin. Microbiol. *38*, 156-164.
654 10.1016/j.mib.2017.05.006.
655 33. Arnold, J., Glazier, J., and Mimee, M. (2023). Genetic Engineering of Resident Bacteria in
656 the Gut Microbiome. Journal of Bacteriology *205*, e00127-00123. 10.1128/jb.00127-23.
657 34. Cervantes-Barragan, L., Chai, J.N., Tianero, M.D., Di Luccia, B., Ahern, P.P., Merriman, J.,
658 Cortez, V.S., Caparon, M.G., Donia, M.S., Gilfillan, S., et al. (2017). Lactobacillus reuteri
659 induces gut intraepithelial CD4(+)CD8alphaalpha(+) T cells. Science *357*, 806-810.
660 10.1126/science.aah5825.

661 35. Zelante, T., Iannitti, R.G., Cunha, C., De Luca, A., Giovannini, G., Pieraccini, G., Zecchi,
662 R., D'Angelo, C., Massi-Benedetti, C., Fallarino, F., et al. (2013). Tryptophan catabolites
663 from microbiota engage aryl hydrocarbon receptor and balance mucosal reactivity via
664 interleukin-22. Immunity *39*, 372-385. 10.1016/j.immuni.2013.08.003.
665 36. Kueck, T., Cassella, E., Holler, J., Kim, B., and Bieniasz, P.D. (2018). The aryl hydrocarbon
666 receptor and interferon gamma generate antiviral states via transcriptional repression.
667 eLife *7*, e38867. 10.7554/eLife.38867.
668 37. Fulcher, J.A., Li, F., Tobin, N.H., Zabih, S., Elliott, J., Clark, J.L., D'Aquila, R., Mustanski,
669 B., Kipke, M.D., Shoptaw, S., et al. (2022). Gut dysbiosis and inflammatory blood markers
670 precede HIV with limited changes after early seroconversion. eBioMedicine *84*.
671 10.1016/j.ebiom.2022.104286.
672 38. Lawrence, B.P., and Vorderstrasse, B.A. (2013). New insights into the aryl hydrocarbon
673 receptor as a modulator of host responses to infection. Semin Immunopathol *35*, 615-626.
674 10.1007/s00281-013-0395-3.
675 39. Torti, M.F., Giovannoni, F., Quintana, F.J., and Garcia, C.C. (2021). The Aryl Hydrocarbon
676 Receptor as a Modulator of Anti-viral Immunity. Front Immunol *12*, 624293.
677 10.3389/fimmu.2021.624293.
678 40. Fischbach, M.A. (2018). Microbiome: Focus on Causation and Mechanism. Cell *174*, 785-
679 790. https://doi.org/10.1016/j.cell.2018.07.038.
680 41. Giovanni, M.Y., Schneider, J.S., Calder, T., and Fauci, A.S. (2021). Refocusing Human
681 Microbiota Research in Infectious and Immune-mediated Diseases: Advancing to the Next
682 Stage. J. Infect. Dis. *224*, 5-8. 10.1093/infdis/jiaa706.
683 42. Wu, M., Zheng, W., Song, X., Bao, B., Wang, Y., Ramanan, D., Yang, D., Liu, R., Macbeth,
684 J.C., Do, E.A., et al. (2024). Gut complement induced by the microbiota combats
685 pathogens and spares commensals. Cell. https://doi.org/10.1016/j.cell.2023.12.036.

686 43. Vujkovic-Cvijin, I., Sortino, O., Verheij, E., Sklar, J., Wit, F.W., Kootstra, N.A., Sellers, B.,
687 Brenchley, J.M., Ananworanich, J., Loeff, M.S.v.d., et al. (2020). HIV-associated gut
688 dysbiosis is independent of sexual practice and correlates with noncommunicable
689 diseases. Nature Communications *11*, 2448. 10.1038/s41467-020-16222-8.
690 44. Dillon, S.M., Lee, E.J., Kotter, C.V., Austin, G.L., Dong, Z., Hecht, D.K., Gianella, S., Siewe,
691 B., Smith, D.M., Landay, A.L., et al. (2014). An altered intestinal mucosal microbiome in
692 HIV-1 infection is associated with mucosal and systemic immune activation and
693 endotoxemia. Mucosal Immunology *7*, 983-994. 10.1038/mi.2013.116.
694 45. McHardy, I.H., Li, X., Tong, M., Ruegger, P., Jacobs, J., Borneman, J., Anton, P., and Braun,
695 J. (2013). HIV Infection is associated with compositional and functional shifts in the rectal
696 mucosal microbiota. Microbiome *1*, 26. 10.1186/2049-2618-1-26.
697 46. Mutlu, E.A., Keshavarzian, A., Losurdo, J., Swanson, G., Siewe, B., Forsyth, C., French,
698 A., DeMarais, P., Sun, Y., Koenig, L., et al. (2014). A Compositional Look at the Human
699 Gastrointestinal Microbiome and Immune Activation Parameters in HIV Infected Subjects.
700 PLOS Pathogens *10*, e1003829. 10.1371/journal.ppat.1003829.
701 47. Abange, W.B., Martin, C., Nanfack, A.J., Yatchou, L.G., Nusbacher, N., Nguedia, C.A.,
702 Kamga, H.G., Fokam, J., Kennedy, S.P., Ndjolo, A., et al. (2021). Alteration of the gut fecal
703 microbiome in children living with HIV on antiretroviral therapy in Yaounde, Cameroon.
704 Scientific Reports *11*, 7666. 10.1038/s41598-021-87368-8.
705 48. Guo, C.J., Allen, B.M., Hiam, K.J., Dodd, D., Van Treuren, W., Higginbottom, S.,
706 Nagashima, K., Fischer, C.R., Sonnenburg, J.L., Spitzer, M.H., and Fischbach, M.A.
707 (2019). Depletion of microbiome-derived molecules in the host using Clostridium genetics.
708 Science *366*. 10.1126/science.aav1282.
709 49. Jin, W.B., Li, T.T., Huo, D., Qu, S., Li, X.V., Arifuzzaman, M., Lima, S.F., Shi, H.Q., Wang,
710 A., Putzel, G.G., et al. (2022). Genetic manipulation of gut microbes enables single-gene

711 interrogation in a complex microbiome. Cell *185*, 547-562 e522.
712 10.1016/j.cell.2021.12.035.
713 50. Chatterjee, D., Zhang, Y., Ngassaki-Yoka, C.D., Dutilleul, A., Khalfi, S., Hernalsteens, O.,
714 Wiche Salinas, T.R., Dias, J., Chen, H., Smail, Y., et al. (2023). Identification of aryl
715 hydrocarbon receptor as a barrier to HIV-1 infection and outgrowth in CD4(+) T cells. Cell
716 Rep *42*, 112634. 10.1016/j.celrep.2023.112634.
717 51. Veiga-Parga, T., Suryawanshi, A., and Rouse, B.T. (2011). Controlling viral immuno-
718 inflammatory lesions by modulating aryl hydrocarbon receptor signaling. PLoS Pathog *7*,
719 e1002427. 10.1371/journal.ppat.1002427.
720 52. Naseri-Nosar, P., Nogalski, M.T., and Shenk, T. (2021). The aryl hydrocarbon receptor
721 facilitates the human cytomegalovirus-mediated G1/S block to cell cycle progression. Proc.
722 Natl. Acad. Sci. U. S. A. *118*. 10.1073/pnas.2026336118.
723 53. Giovannoni, F., Bosch, I., Polonio, C.M., Torti, M.F., Wheeler, M.A., Li, Z., Romorini, L.,
724 Rodriguez Varela, M.S., Rothhammer, V., Barroso, A., et al. (2020). AHR is a Zika virus
725 host factor and a candidate target for antiviral therapy. Nature Neuroscience *23*, 939-951.
726 10.1038/s41593-020-0664-0.
727 54. Quintana, F.J., Basso, A.S., Iglesias, A.H., Korn, T., Farez, M.F., Bettelli, E., Caccamo, M.,
728 Oukka, M., and Weiner, H.L. (2008). Control of Treg and TH17 cell differentiation by the
729 aryl hydrocarbon receptor. Nature *453*, 65-71. 10.1038/nature06880.
730 55. Zhou, Y.H., Sun, L., Chen, J., Sun, W.W., Ma, L., Han, Y., Jin, X., Zhao, Q.X., Li, T., Lu, H.,
731 et al. (2019). Tryptophan Metabolism Activates Aryl Hydrocarbon Receptor-Mediated
732 Pathway To Promote HIV-1 Infection and Reactivation. mBio *10*. 10.1128/mBio.02591-19.
733 56. Veldhoen, M., Hirota, K., Westendorf, A.M., Buer, J., Dumoutier, L., Renauld, J.C., and
734 Stockinger, B. (2008). The aryl hydrocarbon receptor links TH17-cell-mediated
735 autoimmunity to environmental toxins. Nature *453*, 106-109. 10.1038/nature06881.

736 57. Boule, L.A., Burke, C.G., Jin, G.B., and Lawrence, B.P. (2018). Aryl hydrocarbon receptor
737 signaling modulates antiviral immune responses: ligand metabolism rather than chemical
738 source is the stronger predictor of outcome. Sci Rep *8*, 1826. 10.1038/s41598-018-20197-
739 4.
740 58. Higashitani, K., Kanto, T., Kuroda, S., Yoshio, S., Matsubara, T., Kakita, N., Oze, T.,
741 Miyazaki, M., Sakakibara, M., Hiramatsu, N., et al. (2013). Association of enhanced activity
742 of indoleamine 2,3-dioxygenase in dendritic cells with the induction of regulatory T cells in
743 chronic hepatitis C infection. J. Gastroenterol. *48*, 660-670. 10.1007/s00535-012-0667-z.
744 59. Sadeghi, M., Lahdou, I., Daniel, V., Schnitzler, P., Fusch, G., Schefold, J.C., Zeier, M.,
745 Iancu, M., Opelz, G., and Terness, P. (2012). Strong association of phenylalanine and
746 tryptophan metabolites with activated cytomegalovirus infection in kidney transplant
747 recipients. Hum. Immunol. *73*, 186-192. 10.1016/j.humimm.2011.11.002.
748 60. Seok, S.H., Ma, Z.X., Feltenberger, J.B., Chen, H., Chen, H., Scarlett, C., Lin, Z., Satyshur,
749 K.A., Cortopassi, M., Jefcoate, C.R., et al. (2018). Trace derivatives of kynurenine potently
750 activate the aryl hydrocarbon receptor (AHR). J. Biol. Chem. *293*, 1994-2005.
751 10.1074/jbc.RA117.000631.
752 61. Mezrich, J.D., Fechner, J.H., Zhang, X., Johnson, B.P., Burlingham, W.J., and Bradfield,
753 C.A. (2010). An interaction between kynurenine and the aryl hydrocarbon receptor can
754 generate regulatory T cells. J. Immunol. *185*, 3190-3198. 10.4049/jimmunol.0903670.
755 62. Nguyen, N.T., Kimura, A., Nakahama, T., Chinen, I., Masuda, K., Nohara, K., Fujii-
756 Kuriyama, Y., and Kishimoto, T. (2010). Aryl hydrocarbon receptor negatively regulates
757 dendritic cell immunogenicity via a kynurenine-dependent mechanism. Proc. Natl. Acad.
758 Sci. U. S. A. *107*, 19961-19966. 10.1073/pnas.1014465107.
759 63. Opitz, C.A., Litzenburger, U.M., Sahm, F., Ott, M., Tritschler, I., Trump, S., Schumacher,
760 T., Jestaedt, L., Schrenk, D., Weller, M., et al. (2011). An endogenous tumour-promoting

761 ligand of the human aryl hydrocarbon receptor. Nature *478*, 197-203.
762 10.1038/nature10491.
763 64. Boasso, A., Vaccari, M., Fuchs, D., Hardy, A.W., Tsai, W.-P., Tryniszewska, E., Shearer,
764 G.M., and Franchini, G. (2009). Combined Effect of Antiretroviral Therapy and Blockade
765 of IDO in SIV-Infected Rhesus Macaques1. The Journal of Immunology *182*, 4313-4320.
766 10.4049/jimmunol.0803314.
767 65. Cribier, A., Descours, B., Valadão, Ana Luiza C., Laguette, N., and Benkirane, M. (2013).
768 Phosphorylation of SAMHD1 by Cyclin A2/CDK1 Regulates Its Restriction Activity toward
769 HIV-1. Cell Reports *3*, 1036-1043. https://doi.org/10.1016/j.celrep.2013.03.017.
770 66. St Gelais, C., de Silva, S., Hach, J.C., White, T.E., Diaz-Griffero, F., Yount, J.S., and Wu,
771 L. (2014). Identification of cellular proteins interacting with the retroviral restriction factor
772 SAMHD1. J Virol *88*, 5834-5844. 10.1128/jvi.00155-14.
773 67. Love, M.I., Huber, W., and Anders, S. (2014). Moderated estimation of fold change and
774 dispersion for RNA-seq data with DESeq2. Genome Biol *15*, 550. 10.1186/s13059-014-
775 0550-8.
776 68. Cervantes-Barragan, L., Chai, J.N., Tianero, M.D., Di Luccia, B., Ahern, P.P., Merriman, J.,
777 Cortez, V.S., Caparon, M.G., Donia, M.S., Gilfillan, S., et al. (2017). Lactobacillus reuteri
778 induces gut intraepithelial CD4(+)CD8αα(+) T cells. Science *357*, 806-810.
779 10.1126/science.aah5825.
780 69. Goswami, R., Nelson, A.N., Tu, J.J., Dennis, M., Feng, L., Kumar, A., Mangold, J., Mangan,
781 R.J., Mattingly, C., Curtis, A.D., 2nd, et al. (2019). Analytical Treatment Interruption after
782 Short-Term Antiretroviral Therapy in a Postnatally Simian-Human Immunodeficiency
783 Virus-Infected Infant Rhesus Macaque Model. mBio *10*. 10.1128/mBio.01971-19.
784 70. Hübner, W., McNerney, G.P., Chen, P., Dale, B.M., Gordon, R.E., Chuang, F.Y., Li, X.D.,
785 Asmuth, D.M., Huser, T., and Chen, B.K. (2009). Quantitative 3D video microscopy of HIV

786 transfer across T cell virological synapses. Science *323*, 1743-1747.
787 10.1126/science.1167525.
788 71. deCamp, A., Hraber, P., Bailer, R.T., Seaman, M.S., Ochsenbauer, C., Kappes, J.,
789 Gottardo, R., Edlefsen, P., Self, S., Tang, H., et al. (2014). Global panel of HIV-1 Env
790 reference strains for standardized assessments of vaccine-elicited neutralizing antibodies.
791 J Virol *88*, 2489-2507. 10.1128/jvi.02853-13.
792 72. Sarzotti-Kelsoe, M., Bailer, R.T., Turk, E., Lin, C.L., Bilska, M., Greene, K.M., Gao, H.,
793 Todd, C.A., Ozaki, D.A., Seaman, M.S., et al. (2014). Optimization and validation of the
794 TZM-bl assay for standardized assessments of neutralizing antibodies against HIV-1. J
795 Immunol Methods *409*, 131-146. 10.1016/j.jim.2013.11.022.
796 73. Kumar, A., Smith, C.E.P., Giorgi, E.E., Eudailey, J., Martinez, D.R., Yusim, K., Douglas,
797 A.O., Stamper, L., McGuire, E., LaBranche, C.C., et al. (2018). Infant transmitted/founder
798 HIV-1 viruses from peripartum transmission are neutralization resistant to paired maternal
799 plasma. PLOS Pathogens *14*, e1006944. 10.1371/journal.ppat.1006944.
800 74. Murphy, E., Yu, D., Grimwood, J., Schmutz, J., Dickson, M., Jarvis, M.A., Hahn, G., Nelson,
801 J.A., Myers, R.M., and Shenk, T.E. (2003). Coding potential of laboratory and clinical
802 strains of human cytomegalovirus. Proc Natl Acad Sci U S A *100*, 14976-14981.
803 10.1073/pnas.2136652100.
804 75. Kalejta, R.F., Bechtel, J.T., and Shenk, T. (2003). Human cytomegalovirus pp71 stimulates
805 cell cycle progression by inducing the proteasome-dependent degradation of the
806 retinoblastoma family of tumor suppressors. Mol Cell Biol *23*, 1885-1895.
807 10.1128/mcb.23.6.1885-1895.2003.
808 76. Wang, H.-Y., Li, L., Nelson, C.S., Barfield, R., Valencia, S., Chan, C., Muramatsu, H., Lin,
809 P.J.C., Pardi, N., An, Z., et al. (2024). Multivalent cytomegalovirus glycoprotein B
810 nucleoside modified mRNA vaccines did not demonstrate a greater antibody breadth. npj
811 Vaccines *9*, 38. 10.1038/s41541-024-00821-3.

812 77. Heap, J.T., Pennington, O.J., Cartman, S.T., and Minton, N.P. (2009). A modular system
813 for Clostridium shuttle plasmids. J. Microbiol. Methods *78*, 79-85.
814 10.1016/j.mimet.2009.05.004.
815 78. Beghini, F., McIver, L.J., Blanco-Miguez, A., Dubois, L., Asnicar, F., Maharjan, S., Mailyan,
816 A., Manghi, P., Scholz, M., Thomas, A.M., et al. (2021). Integrating taxonomic, functional,
817 and strain-level profiling of diverse microbial communities with bioBakery 3. eLife *10*.
818 10.7554/eLife.65088.
819 79. The UniProt, C. (2023). UniProt: the Universal Protein Knowledgebase in 2023. Nucleic
820 Acids Research *51*, D523-D531. 10.1093/nar/gkac1052.
821
822

823 **FIGURE LEGENDS**

824 **Figure 1. Microbe–phenotype triangulation associated two bacterial taxa with protection**
825 **against SHIV infection. (A)** Schematic of the nonhuman primate study design. Newborn animals
826 were immunized by either an HIV or control vaccine (n = 12/group) at 0, 6, 12 weeks of age.
827 Starting at 15 weeks of age, animals were orally challenged with SHIV weekly until they became
828 infected. Fecal samples were collected just prior to the SHIV challenges for 16S rRNA gene
829 sequencing. **(B)** Distribution of the number of weekly SHIV challenges each monkey received
830 before becoming infected. Bars are colored by regimen groups. **(C)** The different pairwise
831 comparisons used for microbe-phenotype triangulation are depicted. The two bacterial taxa
832 associated with delayed acquisition of SHIV are listed. VAX, animals receiving the HIV vaccine;
833 CTL, animals receiving the control vaccine. **(D–E)** Relative abundance of *L. gasseri* **(D)** and
834 Lachnospiraceae **(E)** in HIV-vaccinated animals that were infected early or late. The bars
835 represent means±SEM. *P<0.05; **P<0.01 by Mann-Whitney U test.

836

837 **Figure 2. Human-derived *L. gasseri* and Lachnospiraceae isolates robustly inhibit HIV**
838 **infection in vitro and ex vivo. (A–B)** Percent inhibition of HIV replication for CCR5-tropic **(A)**
839 and CXCR4-tropic **(B)** strains of HIV in TZM-bl cells treated with the indicated commensal bacteria.
840 ARV, antiretroviral cocktail. **(C)** Percent inhibition of HIV replication in human tonsillar T cells
841 treated with the indicated commensal bacteria. **(D)** Time-of-addition assay results for *C. immunis*
842 and *R. gnavus*. The times depicted for the various viral pathogenesis steps were determined using
843 antiviral drugs targeting each step. RT, reverse transcription; IN, integration. Data are normalized
844 to HIV-infected TZM-bl cells or tonsillar T cells treated with *B. fragilis* **(A–C)** or TZM-bl cells treated
845 with *B. fragilis* at 12 hours after infection with HIV **(D)**. Panels A–D include data from 6, 6, 4, and
846 3 independent experiments, respectively; in panel B, the data for *L. gasseri* 5011 is from 3
847 independent experiments. Data are represented as mean±SEM. ns, not significant; *P<0.05;

848 **P<0.01; ***P<0.001; ****P<0.0001 by one-sample t-tests compared to a mean of 0 and adjusted
849 for multiple comparisons by the Benjamini-Hochberg procedure **(A–C)** or a paired one-way
850 ANOVA with post-hoc Sidak's tests (**D**)**.** See also **Figure S1 and S2**.
851
852 **Figure 3. Commensal bacteria inhibit HIV infection via the ArAT gene.**
853 **(A)** Percent inhibition of HIV replication in TZM-bl cells treated with the indicated fraction of heat-
854 killed *C. immunis* culture. **(B)** Percent inhibition of HIV replication in TZM-bl cells treated with *C.*
855 *immunis* or *C. immunis*ΔArAT. **(C)** Percent inhibition of HIV replication in human tonsillar T cells
856 treated with *C. immunis* or *C. immunis*ΔArAT. **(D)** Time-of-addition assay results for *C. immunis*
857 and *C. immunis*ΔArAT. The times depicted for the various viral pathogenesis steps were
858 determined using antivirals targeting each step. RT, reverse transcription; IN, integration. The data
859 for *C. immunis* are the same as that present in Figure 2D. **(E)** Percent inhibition of HIV replication
860 in TZM-bl cells treated with *B. fragilis*, *L. reuteri*, or *L. reuteri*ΔArAT. Data are normalized to HIV-
861 infected TZM-bl cells or primary T cells treated with *B. fragilis* **(A–C)**, *B. fragilis* added at 12 hours
862 post-infection **(D)**, or HIV-infected TZM-bl cells not treated with bacteria **(E)**. In panels A–E, data
863 are from 5, 4, 4, 3, and 7 independent experiments, respectively. Data are represented as
864 mean±SEM. ns, not significant; *P<0.05; **P<0.01; ***P<0.001; ****P<0.0001 by one-way ANOVA
865 with post-hoc Tukey's tests **(A, E)**, two-sample t-test **(B, C),** or a paired one-way ANOVA with
866 post-hoc Sidak's tests **(D)**. See also **Figure S2 and S3**.
867
868 **Figure 4. Bacterial production of ILA inhibits HIV infection by activating the aryl**
869 **hydrocarbon receptor.**
870 **(A)** Mass spectrometric quantitation of ILA produced by *C. immunis* and *C. immunis*ΔArAT. **(B)**
871 Percent HIV replication in TZM-bl cells treated with the indicated small molecule. Data are
872 normalized to cells treated with DMSO. **(C, D)** Relative expression of *Cdk1* **(C)** and *Cdk*2 **(D)** in

873 HIV-infected TZM-bl cells treated with the indicated bacteria. **(E)** The fecal abundance of the ArAT
874 gene in adults at-risk for HIV who did (case; *n* = 9) or did not acquire HIV (control; *n* = 20). The
875 samples for the cases were obtained before they became HIV-positive. In panels A, C and D, data
876 are from 7, 6, and 6 independent experiments, respectively; in panel B, data are from 3
877 independent experiments for I3A, 5 for ILA, and 4 for FICZ. Data are represented as mean±SEM.
878 ns, not significant; ***P*<0.01, ****P*<0.001; *****P*<0.0001 by two-sample t-test **(A)**, one-sample t-
879 tests compared to a mean of 100 and adjusted by the Benjamini-Hochberg procedure **(B)** or one-
880 way ANOVA with post-hoc Tukey's tests **(C, D)**. The P-value plotted in panel E is calculated by a
881 Mann-Whitney U test.
882
883 **Figure 5. Bacterial ArAT also inhibits CMV replication.**
884 Percent inhibition of CMV replication in ARPE cells treated with Cytogam, *C. immunis*, or *C.*
885 *immunis*ΔArAT. Data are normalized to ARPE cells treated with *B. fragilis*. Data are from 7
886 independent experiments, with bars representing means±SEM. *****P*<0.0001. Asterisks at the top
887 of the graph represent the *P* value obtained when comparing each sample to the control by one-
888 sample t-tests compared to a mean of 0 and adjusted by the Benjamini-Hochberg procedure. The
889 asterisks above the bracket represent the *P* value obtained when comparing *C. immunis* and *C.*
890 *immunis*ΔArAT by a two-sample t-test.
891
892

893 **Supplementary Figure Legends**

894 **Supplementary Figure 1. *C. immunis* and *R. gnavus* inhibit replication of different HIV**
895 **clades, related to Figure 2. (A–C)** Percent inhibition of clade B **(A)**, clade CRF07 **(B)**, and clade
896 C **(C)** HIV replication in TZM-bl cells treated with the indicated commensal bacteria. Data are
897 normalized to cells treated with *B. fragilis*. ARV, antiretroviral cocktail. Data are from 6
898 independent experiments, with bars representing means ± SEM. **P*<0.05; ****P*<0.001;
899 *****P*<0.0001 by one-sample t-tests compared to a mean of 0 and adjusted by the Benjamini-
900 Hochberg procedure.

901

902 **Supplementary Figure 2. The kinetics of HIV pathogenesis are defined by canonical anti-**
903 **HIV drugs, related to Figure 2 and Figure 3**. Time-of-addition assay results for VRC01, an anti-
904 CD4 antibody, enfuvirtide, zidovudine, and raltegravir. Data are normalized to cells treated with
905 DMSO at 12 hours, are from 3 independent experiments, and are represented as means±SEM.
906 RT, reverse transcription; IN, integration. ***P*<0.01; ****P*<0.001; *****P*<0.0001 by one-way ANOVA
907 with post-hoc Sidak's tests.

908

909 **Supplementary Figure 3. Pre-treatment with *C. immunis* or *R. gnavus* is sufficient to inhibit**
910 **HIV replication, related to Figure 3**. Percent inhibition of HIV replication in TZM-bl cells pre-
911 treated with *C. immunis* or *R. gnavus*, washed to remove bacteria, and then infected with HIV.
912 Data are normalized to cells treated with *B. fragilis*, are from 3 independent experiments, and are
913 represented as means±SEM. ***P*<0.01; ****P*<0.001 by one-sample t-tests compared to a mean
914 of 0 and adjusted by the Benjamini-Hochberg procedure.

915

916

Figure 1

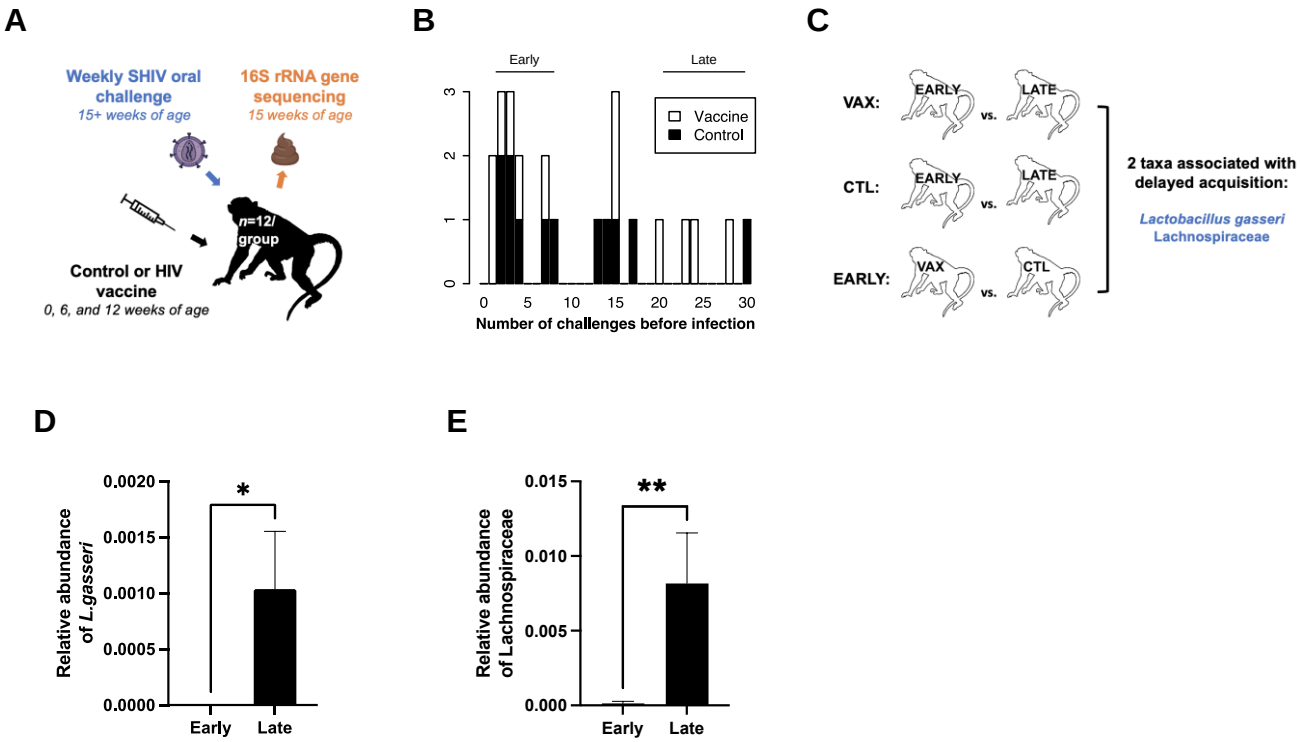
A
Weekly SHIV oral challenge
15+ weeks of age
16S rRNA gene sequencing
15 weeks of age
n=12/ group
Control or HIV vaccine
0, 6, and 12 weeks of age
B
Early
Late
Vaccine
Control
0
1
2
3
0
5
10
15
20
25
30
Number of challenges before infection
C
VAX:
EARLY
vs.
LATE
CTL:
EARLY
vs.
LATE
EARLY:
VAX
vs.
CTL
2 taxa associated with delayed acquisition:
Lactobacillus gasseri
Lachnospiraceae
D
Relative abundance of L.gasseri
0.0020
0.0015
0.0010
0.0005
0.0000
*
Early
Late
E
Relative abundance of Lachnospiraceae
0.015
0.010
0.005
0.000
**
Early
Late

Figure 2

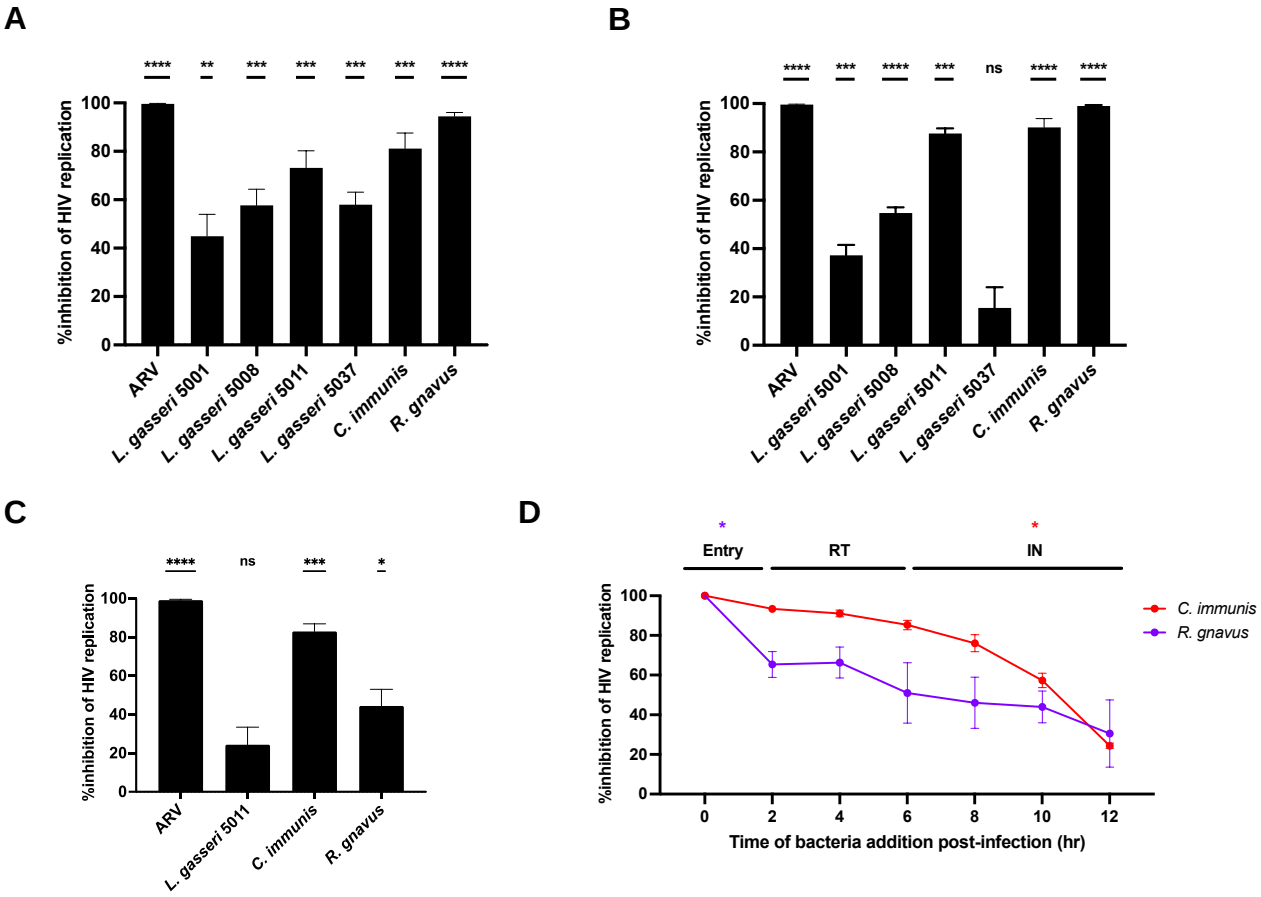
A
%inhibition of HIV replication
0
20
40
60
80
100
****
**
***
***
***
***
****
ARV
L. gasseri 5001
L. gasseri 5008
L. gasseri 5011
L. gasseri 5037
C. immunis
R. gnavus
B
%inhibition of HIV replication
****
***
****
***
ns
****
****
ARV
L. gasseri 5001
L. gasseri 5008
L. gasseri 5011
L. gasseri 5037
C. immunis
R. gnavus
C
%inhibition of HIV replication
****
ns
***
*
ARV
L. gasseri 5011
C. immunis
R. gnavus
D
*
*
Entry
RT
IN
%inhibition of HIV replication
0
2
4
6
8
10
12
Time of bacteria addition post-infection (hr)
C. immunis
R. gnavus

Figure 3

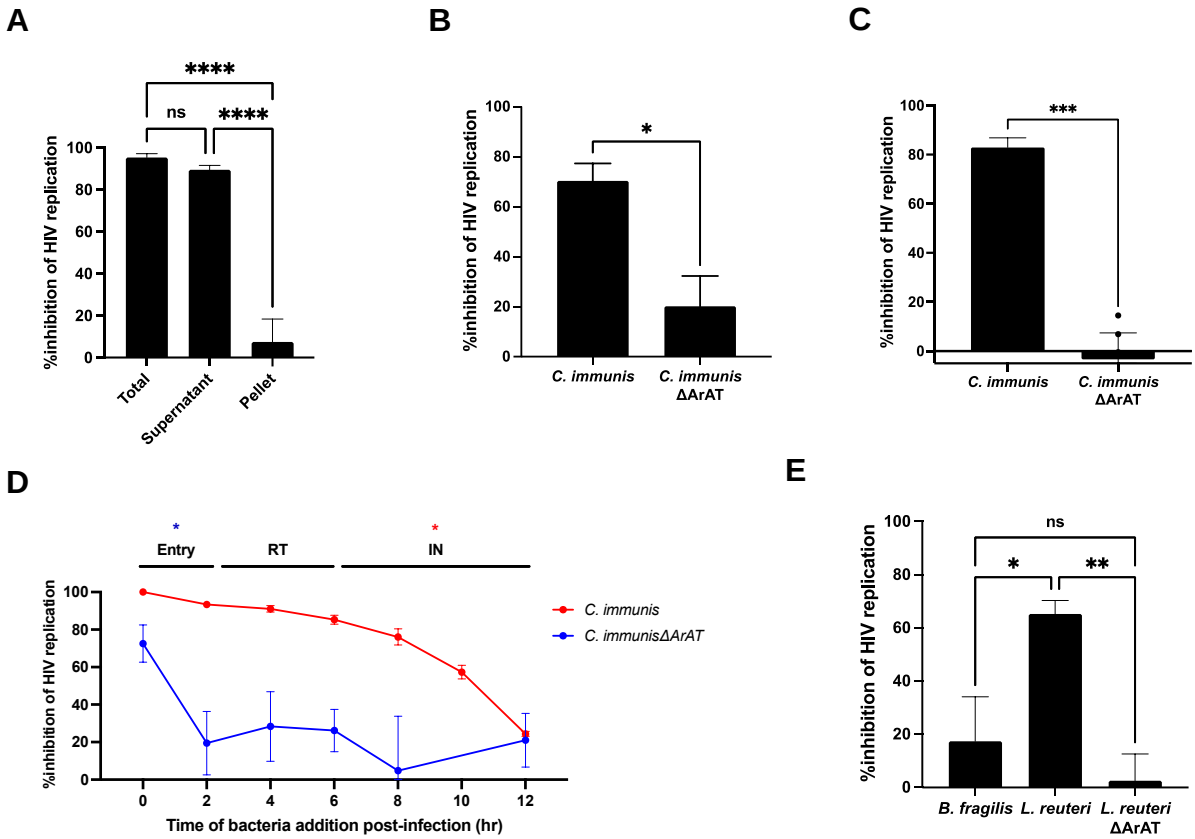
A
****
ns
****
%inhibition of HIV replication
100
80
60
40
20
0
Total
Supernatant
Pellet
B
*
%inhibition of HIV replication
C. immunis
C. immunis ΔArAT
C
***
%inhibition of HIV replication
C. immunis
C. immunis ΔArAT
D
*
*
Entry
RT
IN
%inhibition of HIV replication
C. immunis
C. immunisΔArAT
0
2
4
6
8
10
12
Time of bacteria addition post-infection (hr)
E
ns
*
**
%inhibition of HIV replication
B. fragilis
L. reuteri
L. reuteri ΔArAT

Figure 4

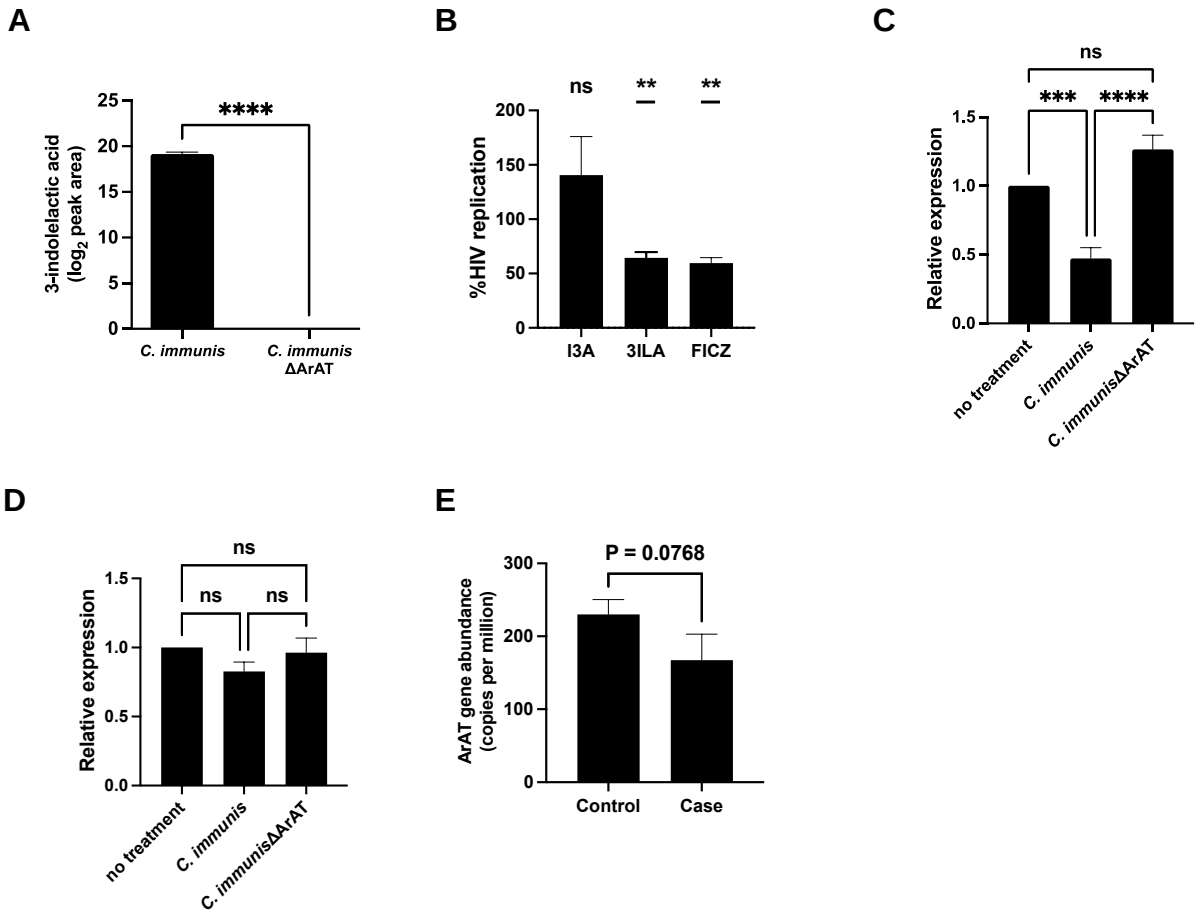
A
3-indolelactic acid
(log2 peak area)
25
20
15
10
5
0
****
C. immunis
C. immunis
ΔArAT
B
%HIV replication
200
150
100
50
0
ns
**
**
I3A
3ILA
FICZ
C
Relative expression
1.5
1.0
0.5
0.0
ns
***
****
no treatment
C. immunis
C. immunisΔArAT
D
Relative expression
1.5
1.0
0.5
0.0
ns
ns
ns
no treatment
C. immunis
C. immunisΔArAT
E
ArAT gene abundance
(copies per million)
300
200
100
0
P = 0.0768
Control
Case

Figure 5

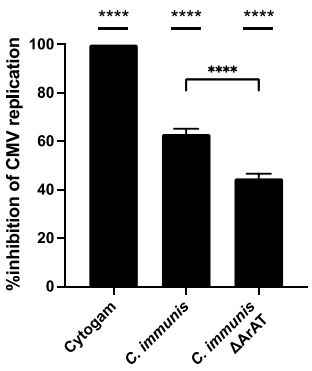
****
****
****
****
%inhibition of CMV replication
100
80
60
40
20
0
Cytogam
C. immunis
C. immunis ΔArAT